

G-Quadruplex Formation in a Putative Coding Region of White Spot Syndrome Virus: Structural and Thermodynamic Aspects

Yoanes Maria Vianney,^[a] Maria Goretti M. Purwanto,^[b] and Klaus Weisz^{*[a]}

White spot disease (WSD) is one of the most devastating viral infections of crustaceans caused by the white spot syndrome virus (WSSV). A conserved sequence *WSSV131* in the DNA genome of WSSV was found to fold into a polymorphic G-quadruplex structure. Supported by two mutant sequences with single G→T substitutions in the third G₄ tract of *WSSV131*, circular dichroism and NMR spectroscopic analyses demonstrate folding of the wild-type sequence into a three-tetrad parallel topology comprising three propeller loops with a major 1:3:1 and a minor 1:2:2 loop length arrangement. A thermodynamic analysis of quadruplex formation by differential scanning calorimetry (DSC) indicates a thermodynamically more stable 1:3:1 loop isomer. DSC also revealed the formation of additional highly stable multimeric species with populations depending on potassium ion concentration.

G-quadruplexes (G4s) are secondary structures of DNA, formed by repeated runs of contiguous guanosine residues. They are widely found throughout different organisms but also occur in viral genomes.^[1,2] G4s have been shown to be involved in the regulation of gene expression, either acting within the regulatory region or the gene itself.^[3–5] Consequently, formation of G-quadruplexes in the viral functional genome may contribute to viral mortality and G-quadruplex-stabilizing ligands may be employed for viral control.^[6–9] The white spot syndrome virus has emerged as one of the most common and most devastating pathogens for farmed crustaceans such as shrimp.^[10,11] WSSV infects all major shrimp species and has caused huge economic losses in the aquaculture industry worldwide due to the lack of effective treatments. Screening the genome of the white spot

syndrome virus (accession number KY827813), we found a conserved sequence with putative G4-forming ability termed *WSSV131* (Figure 1). Its first G tract is located three bases downstream the template strand of the open reading frame (ORF) *WSV131*, encoding a putative yet still unknown protein.^[12,13]

The circular dichroism (CD) spectrum of *WSSV131* exhibits positive and negative amplitudes at ~265 and ~240 nm, typical for a quadruplex with parallel topology and exclusive homopolymers stacking interactions (Figure 2A). The imino proton

name	sequence
<i>WSSV131</i>	5'-TCT <u>GGGAGGG</u> AAGGGGAGGGTTA-3' 1 2 3 4 5 6 7 8 9 10 11 12 13 14 15 16 17 18 19 20 21 22 23
<i>WSSV131-G13T</i>	5'-TCTGGGAGGGAA <u>TGGG</u> AGGGTTA-3'
<i>WSSV131-G16T</i>	5'-TCTGGGAGGGAA <u>GGGT</u> AGGGTTA-3'

Figure 1. *WSSV131* wild-type and mutant sequences; G tracts are underlined and positions 13 and 16 marked in red.

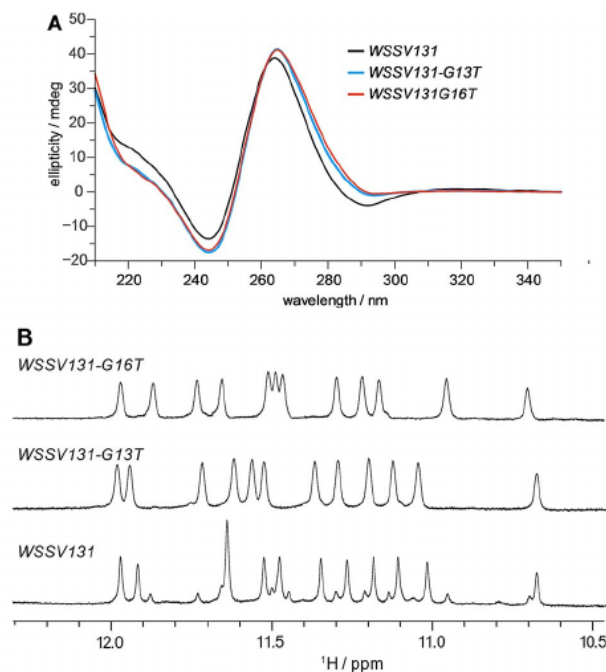


Figure 2. A) CD spectra (20 mM potassium phosphate, pH 7.0, 100 mM KCl, 20 °C) and B) imino proton NMR spectral region (10 mM potassium phosphate, pH 7.0, 25 °C) for *WSSV131* and its G13T and G16T mutants. Note that topologies are conserved under both buffer conditions (Figures S1 and S2 in the Supporting Information).

[a] Y. M. Vianney, Dr. K. Weisz
Institute of Biochemistry
Universität Greifswald
Felix-Hausdorff Str. 4,
17489 Greifswald (Germany)
E-mail: weisz@uni-greifswald.de

[b] Dr. M. G. M. Purwanto
Faculty of Biotechnology
Universitas Surabaya
Kalirungkt Str., Surabaya
60293 (Indonesia)

Supporting information for this article can be found under <https://dx.doi.org/10.1002/cbic.202100064>.

© 2021 The Authors. *ChemBioChem* published by Wiley-VCH GmbH. This is an open access article under the terms of the Creative Commons Attribution License, which permits use, distribution and reproduction in any medium, provided the original work is properly cited.

spectral region of a 1D NMR spectrum for *WSSV131* reveals a set of 12 major imino resonances between 10.5–12.0 ppm characteristic for Hoogsteen hydrogen-bonded guanines arranged in a G-tetrad (Figure 2B). However, additional minor species account for ~30% of the total population. Polymorphism may arise due to the third tract composed of four G residues to potentially form 1:3:1 and 1:2:2 loop isomers. To lock structures to a single loop arrangement, single-site mutants G13T and G16T mimicking 1:3:1 and 1:2:2 loop isomers were evaluated and compared to the wild-type sequence (Figure 1). CD spectra of the mutants featured highly similar signatures typical of a parallel fold (Figure 2A). Notably, imino proton spectral regions for both mutants indicate a single quadruplex comprising twelve imino resonances with their superposition closely matching native *WSSV131* imino signals with the G13T mutant in excess (Figure 2B). These results suggest the presence of a major 1:3:1 and a minor 1:2:2 loop isomer for polymorphic *WSSV131*.

A more detailed NMR structural analysis of the native *WSSV131* sequence employed standard strategies to assign the major loop isomer. Continuous sugar-base NOE connectivities are observed between the 5'-terminal T and the first G-column, between the fourth G-column and the 3' terminus, as well as between guanines constituting the two central G tracts (Figure 3A). Two prominent crosspeaks in the H8/H1'/H5 spectral region observed at long but also shorter mixing times are identified as A11 H8-H1' and C2 H6-H5 contacts through a ^1H , ^{13}C HSQC experiment (Figure S3). Imino-H8 and imino-imino NOE contacts identified guanines involved in G-tetrad formation (Figure 3B, C). There is no indication of any *syn*-guanine

within the four G tracts in the NOESY spectra in line with the observation of exclusively upfield-shifted guanine ^{13}C resonances in the HSQC spectrum characteristic for *anti* conformers (Figure S3). The all-*anti* G-quadruplex matches a parallel topology with G-columns linked by three propeller-type loops.

Intra-tetrad H8-H1 crosspeaks determine the polarity of the G-tetrads, that is, the direction when going from H-bond donor to H-bond acceptor (Figure 3C). Thus, polarities of 5'-tetrad, central, and 3'-tetrad follow G4→G8→G14→G18, G5→G9→G15→G19, and G6→G10→G16→G20, respectively. Polarity is additionally confirmed by typical imino-imino NOE contacts (Figure 3B). Strong crosspeaks connect sequential Gs within the same G tract. In addition, intra-tetrad crosspeaks can be seen between neighboring G columns, for example, G10-G6 and G20-G6, and inter-tetrad contacts connect imino protons in adjacent tetrads, such as, G9-G6 and G10-G15.

There is also a weak NOE crosspeak between A7 H8 of the first propeller loop and preceding G6 H2'. Likewise, residues of the second propeller loop can be identified through NOE walks based on H8/H6-H1'/H2'/H3' contacts from A11 through G13. Another weak sequential contact from G16 H2' to A17 H8 of the third propeller loop also allows assignment of G16 as being the last residue of the third column (Figure S4). Taken together, experimental findings clearly confirm a major *WSSV131* G4 with parallel topology and a central 3-nt propeller loop (Figure 4, for a compilation of chemical shifts, see Table S1). A corresponding more detailed 2D NMR spectral analysis on both G13T and G16T mutants confirmed their parallel fold and the same 1:3:1 loop arrangement for *WSSV131*-G13T as identified for the major species of the wild-type sequence (Figure S5 and S6).

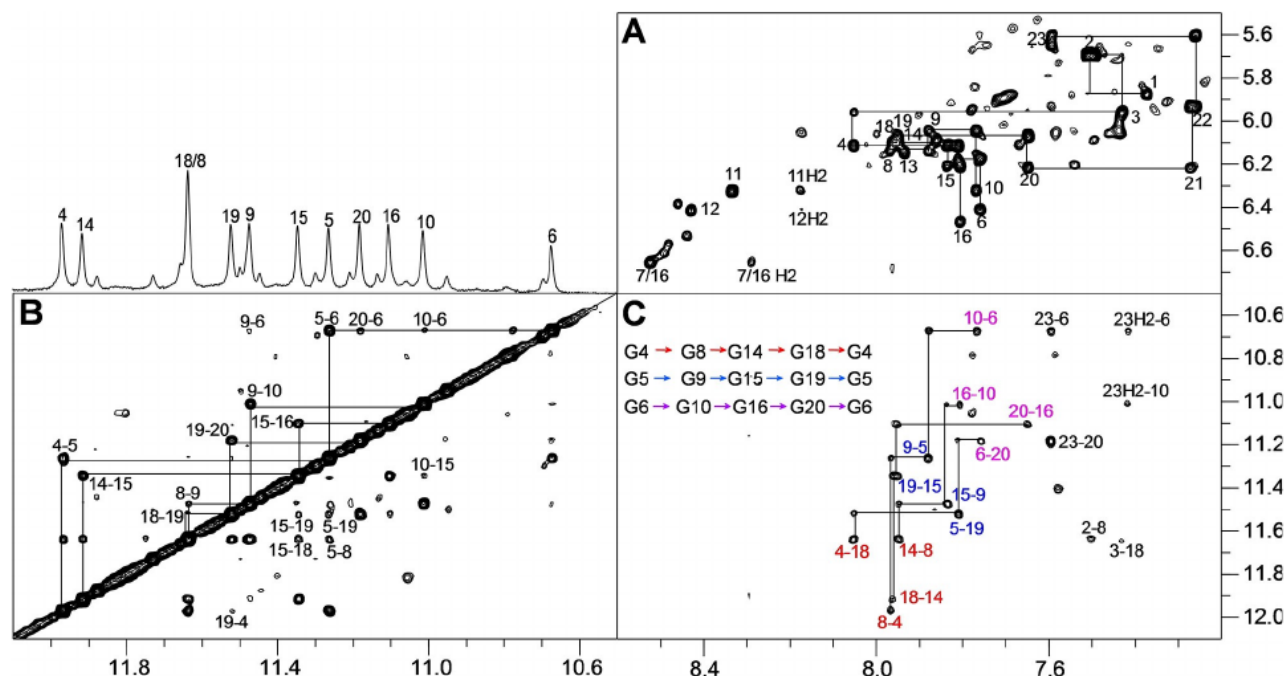


Figure 3. 2D NOE spectral regions of *WSSV131* acquired with a 300 ms mixing time at 25 °C. A) H6/H8(ω_2)-H1'/H5(ω_1) spectral region with continuous NOE walks along G tracts and 5'- and 3'-overhang sequences. B) Imino-imino crosspeaks with sequential connectivities traced along the G tracts. C) Intra- and inter-tetrad H8(ω_2)-imino(ω_1) crosspeaks; tetrad polarities as determined from intra-tetrad NOE contacts (marked in red for the 5'-tetrad, in blue for the central tetrad, and in magenta for the 3'-tetrad) are given in the inset.

Initial UV melting studies on the *WSSV131* G13T and G16T mutants, each forming a single loop isomer, revealed slow kinetics of (un)folding at 10 mM K^+ whereas at 120 mM K^+ melting profiles shifted to temperatures too high for the observation of a well-defined high-temperature baseline within the temperature window accessible (not shown). To nevertheless obtain information on their folding thermodynamics, quadruplex formation was analyzed by DSC in a pressurized cell

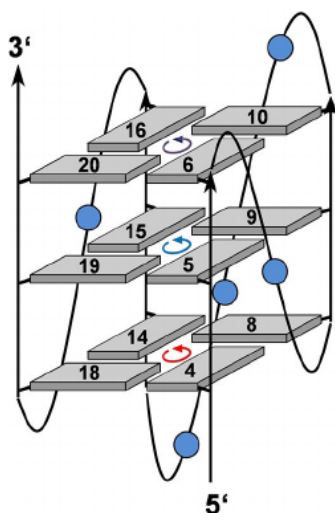


Figure 4. Topology of the *WSSV131* major quadruplex species with tetrad polarities indicated and loop residues represented by circles; residues of the G-core are numbered.

allowing sample heating up to 110 °C without irreversible DNA decomposition. Thermodynamic equilibrium upon heating was verified for both sequences by a match in melting profiles determined with two different heating rates (not shown). After proper baseline correction, DSC data were fitted with a non-two-state model assuming negligible changes in molar heat capacity $\Delta C_p^{[14]}$ to yield T_m as well as calorimetric and van't Hoff molar enthalpies ΔH_{cal}° and ΔH_{vH}° (Figure 5, Table S2).^[15]

In a buffer solution with 120 mM K^+ the major *WSSV131-G13T* quadruplex exhibits a T_m of 68.1 °C, 3.4 °C higher than that of the *WSSV131-G16T* mutant. The higher melting 1:3:1 propeller loop arrangement of *WSSV131-G13T* agrees with systematic studies on the length of propeller loops, reporting a propensity of short first and third loops with a longer central loop.^[16] Interestingly, the less favored *WSSV131-G16T* quadruplex shows another high-temperature transition centered at 103 °C but not fully completed within the experimental temperature range. To shift transitions towards lower temperatures, DSC measurements were also performed in solutions with 90 mM K^+ . Again, in contrast to *WSSV131-G13T* the G16T mutant exhibits an additional high-temperature transition shifted to 99.3 °C but with noticeably reduced height. Based primarily on gel electrophoresis and size exclusion chromatography, high-melting multimeric species have previously been suggested to coexist in particular for parallel-stranded quadruplexes with short loops.^[17–20] However, they have not been observed and characterized by calorimetric methods so far. Taking into account a growing population and faster folding of multimers with increasing K^+ concentration, ΔH_{cal}° for the monomer

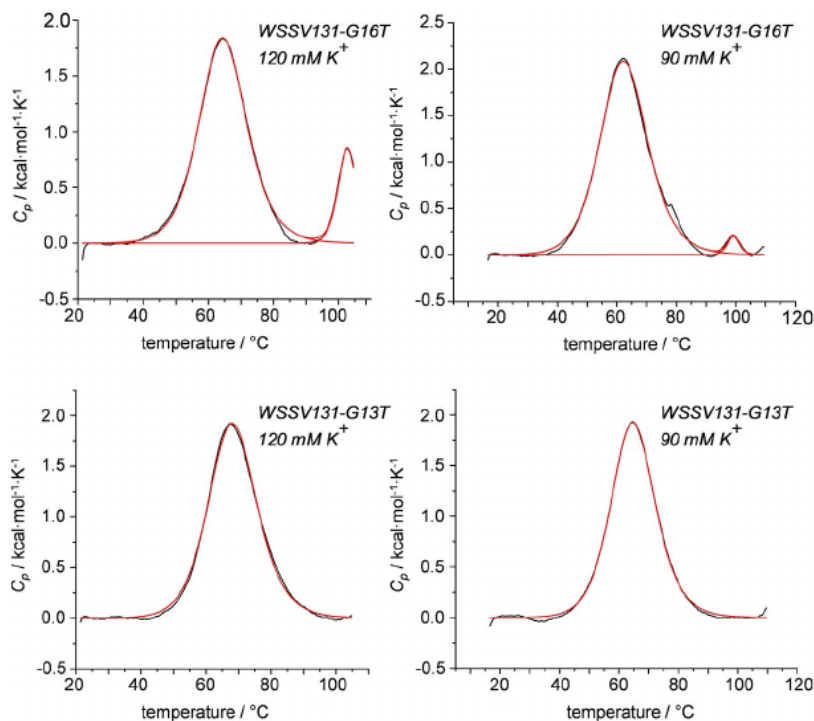


Figure 5. Representative DSC thermograms with a 0.5 °C/min heating rate of *WSSV131* sequences (50 μ M). Melting profiles for *WSSV131-G16T* (top) in the presence of 120 mM K^+ (left) and 90 mM K^+ (right). Melting profiles for *WSSV131-G13T* (bottom) in the presence of 120 mM K^+ (left) and 90 mM K^+ (right). Fitted curves based on a non-two-state model with $\Delta H_{cal}^\circ \neq \Delta H_{vH}^\circ$ are shown in red.

transition at lower temperature is expected to be significantly underestimated in line with a $\Delta H_{\text{vH}}^{\circ}/\Delta H_{\text{cal}}^{\circ} > 1$ in a 120 mM K^{+} buffer. On the other hand, the small population of multimers at 90 mM K^{+} does hardly compromise $\Delta H_{\text{cal}}^{\circ}$ for *WSSV131-G16T*, yielding a $\Delta H_{\text{vH}}^{\circ}/\Delta H_{\text{cal}}^{\circ}$ ratio of about 1 in agreement with a two-state melting transition for the monomer. Because $\Delta H_{\text{vH}}^{\circ}$ is independent of concentration and only depends on the shape of the DSC curve, $\Delta H_{\text{vH}}^{\circ}$ is expected to provide a reliable value for the enthalpy of (un)folding given a two-state transition under equilibrium conditions. With a $\Delta H_{\text{vH}}^{\circ}$ of -47.0 and -46.1 kcal/mol for *WSSV131-G13T* and *WSSV131-G16T* at 120 mM K^{+} as well as -45.9 and -42.9 kcal/mol at 90 mM K^{+} , folding of the more stable G13T mutant seems more exothermic by 1 and 3 kcal/mol. It should also be noted that despite observation of only one DSC transition, $\Delta H_{\text{vH}}^{\circ}/\Delta H_{\text{cal}}^{\circ}$ was found to be > 1 under both salt conditions for *WSSV131-G13T*. This strongly suggests formation of corresponding multimers with even higher thermal stability when compared to those of *WSSV131-G16T*, escaping their detection in the DSC experiment. Indeed, formation of higher-order assemblies for both G16T and G13T mutant sequences are also indicated by native gel electrophoresis experiments in a 90 mM K^{+} buffer (Figure S7).

Taken together, a well-defined parallel quadruplex, highly stable under physiological salt conditions, is formed in a sequence located downstream of a putative coding region in the WSSV viral genome. Such a G4 could possibly be used to regulate viral gene expression and offers the opportunity to ultimately control WSSV infection through the use of G4-binding and G4-stabilizing ligands. Detection and characterization of such G4-prone sequences in the viral genome open new avenues for the target design of antiviral drugs directed against WSSV in crustacean farming.

Acknowledgements

This work was supported by the Deutsche Forschungsgemeinschaft (INST 292/138-1). Open access funding enabled and organized by Projekt DEAL.

Conflict of Interest

The authors declare no conflict of interest.

Keywords: G-quadruplexes · NMR spectroscopy · thermodynamics · white spot syndrome virus

- [1] V. S. Chambers, G. Marsico, J. M. Boutell, M. Di Antonio, G. P. Smith, S. Balasubramanian, *Nat. Biotechnol.* **2015**, *33*, 877–881.
- [2] M. Metifiot, S. Amrane, S. Litvak, M. L. Andreola, *Nucleic Acids Res.* **2014**, *42*, 12352–12366.
- [3] K. Derecka, G. D. Balkwill, T. P. Garner, C. Hodgman, A. P. F. Flint, M. S. Searle, *Biochemistry* **2010**, *49*, 7625–7633.
- [4] P. Zizza, C. Cingolani, S. Artuso, E. Salvati, A. Rizzo, C. D'Angelo, M. Porru, B. Pagano, J. Amato, A. Randazzo, E. Novellino, A. Stoppacciaro, E. Gilson, G. Stassi, C. Leonetti, A. Biroccio, *Nucleic Acids Res.* **2016**, *44*, 1579–1590.
- [5] A. Siddiqui-Jain, C. L. Grand, D. J. Bearss, L. H. Hurley, *Proc. Natl. Acad. Sci. USA* **2002**, *99*, 11593–11598.
- [6] R. Perrone, E. Butovskaya, D. Daelemans, G. Palù, C. Pannecouque, S. N. Richter, *J. Antimicrob. Chemother.* **2014**, *69*, 3248–3258.
- [7] S. R. Wang, Q. Y. Zhang, J. Q. Wang, X. Y. Ge, Y. Y. Song, Y. F. Wang, X. D. Li, B. S. Fu, G. H. Xu, B. Shu, P. Gong, B. Zhang, T. Tian, X. Zhou, *Cell Chem. Biol.* **2016**, *23*, 1113–1122.
- [8] S. R. Wang, Y. Q. Min, J. Q. Wang, C. X. Liu, B. S. Fu, F. Wu, L. Y. Wu, Z. X. Qiao, Y. Y. Song, G. H. Xu, Z. G. Wu, G. Huang, N. F. Peng, R. Huang, W. X. Mao, S. Peng, Y. Q. Chen, Y. Zhu, T. Tian, X. L. Zhang, X. Zhou, *Sci. Adv.* **2016**, *2*, e1501535.
- [9] E. Butovskaya, P. Soldà, M. Scalabrin, M. Nadai, S. N. Richter, *ACS Infect. Dis.* **2019**, *5*, 2127–2135.
- [10] A. Sánchez-Paz, *Vet. Res.* **2010**, *41*, 43.
- [11] M. Lillehammer, R. Banger, M. Salazar, S. Vela, E. C. Erazo, A. Suarez, J. Cock, M. Rye, N. A. Robinson, *Sci. Rep.* **2020**, *10*, 20571.
- [12] Y. Han, F. Li, L. Xu, F. Yang, *Vet. Res.* **2017**, *48*, 1–11.
- [13] Z. Li, F. Li, Y. Han, L. Xu, F. Yang, *J. Virol.* **2016**, *90*, 842–850.
- [14] B. Pagano, A. Randazzo, I. Fotticchia, E. Novellino, L. Petraccone, C. Giancola, *Methods* **2013**, *64*, 43–51.
- [15] J. B. Chaires, *Biophys. Chem.* **1997**, *64*, 15–23.
- [16] P. A. Rachwal, I. S. Findlow, J. M. Werner, T. Brown, K. R. Fox, *Nucleic Acids Res.* **2007**, *35*, 4214–4222.
- [17] H. T. Le, M. C. Miller, R. Buscaglia, W. L. Dean, P. A. Holt, J. B. Chaires, J. O. Trent, *Org. Biomol. Chem.* **2012**, *10*, 9393–9404.
- [18] N. Smargiasso, F. Rosu, W. Hsia, P. Colson, E. S. Baker, M. T. Bowers, E. De Pauw, V. Gabelica, *J. Am. Chem. Soc.* **2008**, *130*, 10208–10216.
- [19] V. Rauser, E. Weinhold, *ChemBioChem* **2020**, *21*, 2445–2448.
- [20] A. Guédin, J. Gros, P. Alberti, J. L. Mergny, *Nucleic Acids Res.* **2010**, *38*, 7858–7868.

Manuscript received: February 11, 2021

Revised manuscript received: March 4, 2021

Accepted manuscript online: March 12, 2021

Version of record online: April 6, 2021

Front Cover:

P. 't Hart, H. Waldmann et al.

Biochemical Investigation of the Interaction of pICln, RioK1 and COPR5 with the PRMT5-MEP50 Complex





Ads by Google

[Stop seeing this ad](#) [Why this ad?](#)

ChemBioChem

COUNTRY

Germany

 Universities and research institutions in Germany

SUBJECT AREA AND CATEGORY

Biochemistry, Genetics and Molecular Biology

[Biochemistry](#)
[Molecular Biology](#)
[Molecular Medicine](#)[Chemistry](#)[Organic Chemistry](#)

PUBLISHER

Wiley-VCH Verlag

H-INDEX

126

PUBLICATION TYPE

Journals

ISSN

14394227, 14397633

COVERAGE

2000-2020

INFORMATION

[Homepage](#)[How to publish in this journal](#)chembiochem@wiley-vch.de

Ads by Google

[Stop seeing this ad](#) [Why this ad?](#)

SCOPE

ChemBioChem (Impact Factor 2018: 2.641) publishes important breakthroughs across all areas at the interface of chemistry and biology, including the fields of chemical biology, bioorganic chemistry, bioinorganic chemistry, synthetic biology, biocatalysis, bionanotechnology, and biomaterials. It is published on behalf of Chemistry Europe, an association of 16 European chemical societies, and supported by the Asian Chemical Editorial Society (ACES).

 [Join the conversation about this journal](#)

Ads by Google

[Stop seeing this ad](#) [Why this ad?](#)

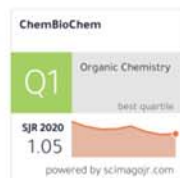
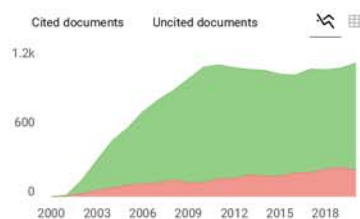
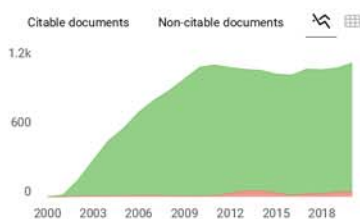
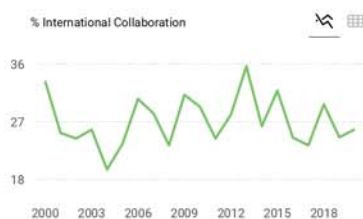
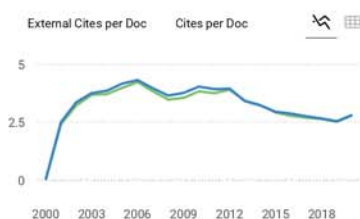
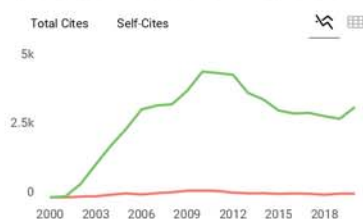
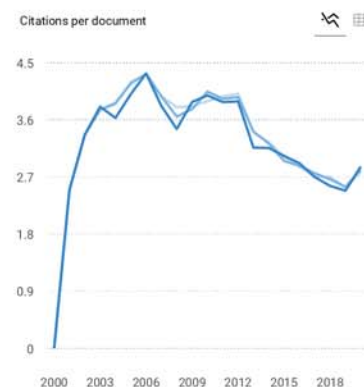
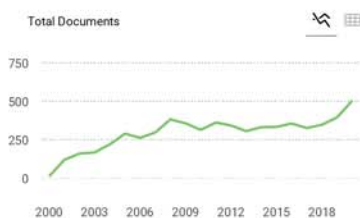
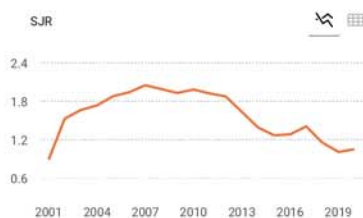
Ads by Google

[Stop seeing this ad](#)
[Why this ad?](#)

FIND SIMILAR JOURNALS

options

Rank	Journal Name	Country	Similarity
1	ACS Chemical Biology	USA	81%
2	Current Opinion in Chemical Biology	GBR	79%
3	Chemical Reviews	USA	76%
4	ACS Central Science	USA	75%
5	Chimia	CHE	74%



Show this widget in your own website

Just copy the code below and paste within your html code:

```
<a href="https://www.scimagojr.com" data-bbox="193 726 294 737">
```

SCImago Graphica

Explore, visually communicate and make sense of data with our **new free tool**.

Get it



Ads by Google

[Stop seeing this ad](#)
[Why this ad?](#)

Metrics based on Scopus® data as of April 2021

Leave a comment

Name

Email

(will not be published)

 I'm not a robot reCAPTCHA
Privacy - Terms**Submit**

The users of Scimago Journal & Country Rank have the possibility to dialogue through comments linked to a specific journal. The purpose is to have a forum in which general doubts about the processes of publication in the journal, experiences and other issues derived from the publication of papers are resolved. For topics on particular articles, maintain the dialogue through the usual channels with your editor.

Developed by:



Powered by:



Follow us on @ScimagoJR

Scimago Lab, Copyright 2007-2020. Data Source: Scopus®

EST MODUS IN REBUS
Scimago (Online) 1.1.100



Source details

ChemBioChem

Scopus coverage years: from 2000 to Present

Publisher: Wiley-Blackwell

ISSN: 1439-4227 E-ISSN: 1439-7633

Subject area: Chemistry: Organic Chemistry Biochemistry, Genetics and Molecular Biology: BiochemistryBiochemistry, Genetics and Molecular Biology: Molecular Biology [View all](#) ▼

Source type: Journal

CiteScore 2020

4.7

SJR 2020

1.050

SNIP 2020

0.681[View all documents](#) >[Set document alert](#)[Save to source list](#) [Source Homepage](#)[CiteScore](#) [CiteScore rank & trend](#) [Scopus content coverage](#)

i Improved CiteScore methodology



CiteScore 2020 counts the citations received in 2017-2020 to articles, reviews, conference papers, book chapters and data papers published in 2017-2020, and divides this by the number of publications published in 2017-2020. [Learn more](#) >

CiteScore 2020 ▼

$$4.7 = \frac{6,902 \text{ Citations } 2017 - 2020}{1,463 \text{ Documents } 2017 - 2020}$$

Calculated on 05 May, 2021

CiteScoreTracker 2021 ⓘ

$$4.9 = \frac{7,272 \text{ Citations to date}}{1,470 \text{ Documents to date}}$$

Last updated on 05 October, 2021 • Updated monthly

CiteScore rank 2020 ⓘ

Category	Rank	Percentile
Chemistry		
└ Organic Chemistry	#65/185	65th
Biochemistry, Genetics and Molecular Biology		
└ Biochemistry	#193/415	53rd
Biochemistry, Genetics and Molecular Biology		
└ Biochemistry	#217/382	43rd

[View CiteScore methodology](#) > [CiteScore FAQ](#) > [Add CiteScore to your site](#) ↗

About Scopus

[What is Scopus](#)
[Content coverage](#)
[Scopus blog](#)
[Scopus API](#)
[Privacy matters](#)

Language

[日本語に切り替える](#)
[切换到简体中文](#)
[切换到繁體中文](#)
[Русский язык](#)

Customer Service

[Help](#)
[Contact us](#)

ELSEVIER

[Terms and conditions](#) ↗ [Privacy policy](#) ↗

Copyright © Elsevier B.V. ↗. All rights reserved. Scopus® is a registered trademark of Elsevier B.V.

We use cookies to help provide and enhance our service and tailor content. By continuing, you agree to the use of cookies.

 RELX

Editorial Advisory Board

Chairs



Thomas Carell
Ludwig-Maximilians-
Universität München



Donald Hilvert
ETH Zürich



Barbara Imperiali
Massachusetts Institute
of Technology, Cambridge

Members

Yasuhisa Asano

Toyama Prefectural University

Hiroyuki Asanuma

Nagoya University

Ashraf Brik

Technion, Haifa

Pimchai Chaipen

Vidyasirimedhi Institute of Science and
Technology

Abhishek Chatterjee

Boston College

Peng Chen

Peking University

Philip Cole

Harvard University

David Craik

University of Queensland, Brisbane

Craig Crews

Yale University

Yael David

Memorial Sloan Kettering Cancer
Institute

Alexander Deiters

University of Pittsburgh

Neal Devaraj

University of California, San Diego

Chunhai Fan

Shanghai Institute of Applied Physics,
CAS

Dorothea Fiedler

Leibniz-Institut für Molekulare
Pharmakologie

Early Career Members

Maria (Masha) Babak

City University of Hong Kong

Claudia Bonfio

MRC Laboratory of Molecular Biology

George Burslem

University of Pennsylvania

Prinessa Chellan

Stellenbosch University

Anne Conibear

University of Queensland, Brisbane

Nina Hartrampf

Universität Zürich

Guifang Jia

Peking University

Shixian Lin

Zhejiang University

Clemens Mayer

Universiteit Groningen

Pablo Ivan Nikel

Danmarks Tekniske Universitet

Denise Okafor

Pennsylvania State University

Yuan Qiao

Nanyang Technological University

Tamara Reyes Robles

Princeton University


Ishu Saraogi

IISER Bhopal


Cathleen Zeymer

Technische Universität München


Beat Fierz

 Ecole polytechnique fédérale de
Lausanne


Marc Fontecave

 Collège de France, Paris


Gilles Gasser

 Chimie ParisTech


Tom Grossmann

 VU University Amsterdam

Christian Hackenberger

 Leibniz-Institut für Molekulare
Pharmakologie


Howard Hang

 Scripps Research


Jennifer Heemstra

 Emory University, Atlanta


Piet Herdewijn

 Katholieke Universiteit Leuven


Christian Hertweck

 Leibniz-Institut für Naturstoffforschung
und Infektionsbiologie


Claudia Höbartner

 Georg-August-Universität Göttingen


Michal Hocek

 Ústav organické chemie a biochemie AV
ČR, Prague


Albert Jeltsch

 Universität Stuttgart


Knud Jørgen Jensen

 Københavns Universitet


Jesús Jiménez-Barbero

 CIC bioGUNE

Kai Johnsson

 MPI für medizinische Forschung,
Heidelberg


Stephanie Kath-Schorr

 Universität zu Köln

Romas Kazlauskas

 University of Minnesota, Twin Cities


Stephen Kent

 University of Chicago


Niveen Khashab

 King Abdullah University of Science and
Technology


Yamuna Krishnan

 University of Chicago

Joana Kowalska

 Uniwersytet Warszawski


Hilal Lashuel

 Ecole polytechnique fédérale de
Lausanne


Jun-Seok Lee

 Korea University, Seoul


Edward Lemke

 IMB Mainz


Dongsheng Liu

 Tsinghua University, Beijing


José Luis Mascareñas

 Universidad de Santiago


Stefan Matile

 Université de Genève


Ronald Micura

 Universität Innsbruck

Antonio Molinaro


 Università degli Studi di Napoli Federico II

Henning Mootz

 Westfälische Wilhelms-Universität

Münster

May Morris

 Institut des Biomolécules Max


Mousseron

Rolf Müller


 Helmholtz-Institut für Pharmazeutische

Forschung Saarland


Hiroshi Murakami

 Nagoya University

Alison Narayan


 University of Michigan

Sarah O'Connor


 Max-Planck-Institut für Chemische

Ökologie


Herman Overkleeft

 Universiteit Leiden

Jörn Piel

 ETH Zürich


Oliver Plettenburg

 Helmholtz-Zentrum München

Liliana Quintanar

 Cinvestav

Raphaël Rodriguez

 Institut Curie

Carsten Schultz

 EMBL

Harald Schwalbe


 Goethe-Universität Frankfurt

Peter Seeberger

 Max-Planck-Institut für Kolloid- und

Grenzflächenforschung

Injae Shin

 Yonsei University


Stephan Sieber

 Technische Universität München


Hanadi Sleiman

 McGill University, Montréal


Hiroaki Suga

 University of Tokyo


Hiroshi Sugiyama

 Kyoto University


[Weihong Tan](#)

 Shanghai Jiao Tong University


[Dirk Trauner](#)

 New York University

[Wilfred van der Donk](#)

 University of Illinois, Urbana-Champaign


[Sandeep Verma](#)

 Indian Institute of Technology, Kanpur

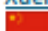
[Itamar Willner](#)

 Hebrew University, Jerusalem

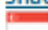
[Nicolas Winssinger](#)

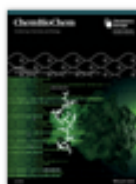
 Université de Genève

[Xuehai Yan](#)

 Chinese Academy of Sciences, Beijing

[Shao Q. Yao](#)

 National University of Singapore



Volume 22, Issue 11

Pages: 1852-2009
June 2, 2021

[◀ Previous Issue](#) | [Next Issue ▶](#)

[☰ GO TO SECTION](#)

[✉ Export Citation\(s\)](#)

Cover Pictures

[🔓 Free Access](#)

Front Cover: Biochemical Investigation of the Interaction of pICln, RioK1 and COPRS with the PRMT5-MEP50 Complex (ChemBioChem 11/2021)

Adrian Krzyzanowski, Dr. Raphael Gasper, Dr. H  l  ne Adihou, Dr. Peter 't Hart, Prof. Dr. Herbert Waldmann

Pages: 1852 | First Published: 04 June 2021



Aligning the adaptor protein sequences: The image shows all sequences derived from PRMT5 adaptor proteins RioK1, pICln and COPRS, that were tested. The consensus sequence GQF[D/E]DA[E/D] was identified, synthesized, and found to bind potently to PRMT5, highlighted as white sequence parts at the highest affinity binding peptides. White alanines represent the sequences, where the mutation to alanine reduced the binding between peptide and PRMT5 the most. Protein truncation and the crystal structure of PRMT5 in complex with a RioK1 derived peptide confirmed the binding and illuminated a novel protein-protein interaction site on the TIM-barrel domain. More information can be found in the Communication by P. 't Hart, H. Waldmann et al.

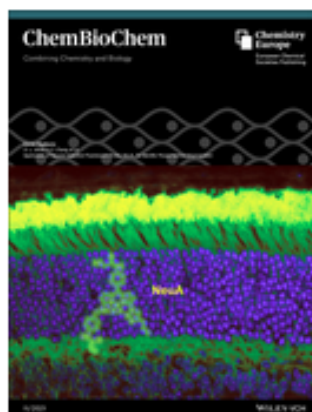
[Abstract](#) | [Full text](#) | [PDF](#) | [Request permissions](#)

[🔓 Free Access](#)

Cover Feature: Application of Neuron-Selective Fluorescent Probe, NeuA, To Identify Mouse Retinal Degeneration (ChemBioChem 11/2021)

Dr. Sung-jin Park, Queenie Tan Shu Woon, Dr. Jun Cheng Er, Dr. Bernice H. Wong, Xiao Liu, Dr. Nam-Young Kang, Dr. Veluchamy A. Barathi, Prof. David L. Silver, Prof. Young-Tae Chang

Pages: 1853 | First Published: 04 June 2021



The newly developed NeuA stains live neurons, such as photoreceptor cells in the retina. The cover feature picture shows the NeuA-stained retina in the cross cryosection after tail vein injection. NeuA highly stains the outer segment layer and cell bodies of photoreceptor cells and some bipolar cells (green). Nuclei were stained with DAPI (blue). With this characteristic, this study demonstrated that NeuA distinguishes between healthy and photoreceptor degenerate retinas as an *in vivo* application. More information can be found in the Communication by D. L. Silver, Y.-T. Chang et al.

[Abstract](#) | [Full text](#) | [PDF](#) | [Request permissions](#)

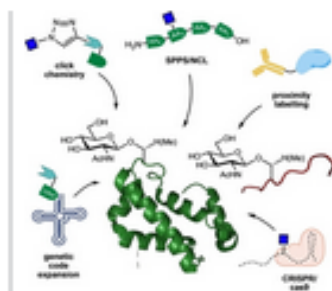
Reviews

Very Important Paper

Chemical Synthesis and Biological Applications of *O*-GlcNAcylated Peptides and Proteins

Jessica M. Groeneveld, Daniel J. Corey, Prof. Charlie Fehli

Pages: 1854-1870 | First Published: 15 January 2021



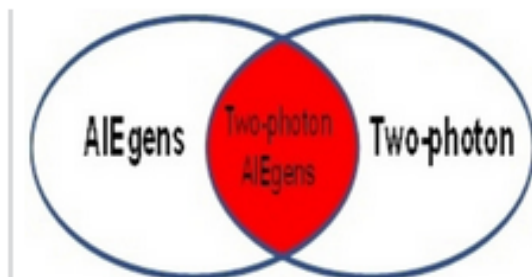
Sugar modifications on proteins enable cells to respond quickly to environmental cues. We review the plethora of chemical strategies to access precise glycoforms of *O*-GlcNAc peptides and full proteins and explore the translational use of synthetic *O*-GlcNAc glycopeptides and glycoproteins as biomarkers, mechanistic probes, and therapeutics. Synthetic *O*-GlcNAc glycobiology is poised to rapidly identify roles in chronic and infectious disease.

[Abstract](#) | [Full text](#) | [PDF](#) | [References](#) | [Request permissions](#)

Recent Advances in Two-Photon AIEgens and Their Application in Biological Systems

Dr. Yandong Dou, Prof. Qing Zhu, Dr. Kui Du

Pages: 1871-1883 | First Published: 04 January 2021



Improving potential: Two-photon AIEgen probes have attracted a lot of attention due to their advantages of large penetration depth, little light damage, dark field imaging and target excitation. This paper reviews the most representative two-photon imaging technology of the past five years, and discusses its great application potential in the field of biological imaging.

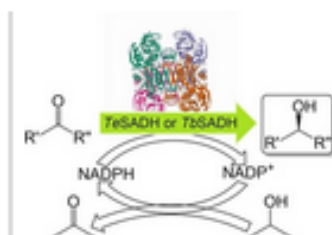
[Abstract](#) | [Full text](#) | [PDF](#) | [References](#) | [Request permissions](#)

Minireviews

Secondary Alcohol Dehydrogenases from *Thermoanaerobacter pseudoethanolicus* and *Thermoanaerobacter brockii* as Robust Catalysts

Prof. Musa M. Musa, Prof. Claire Vielle, Prof. Robert S. Phillips

Pages: 1884-1893 | First Published: 17 February 2021



Scope and selectivity: Recent efforts to expand the substrate scope and tune the enantioselectivity of secondary ADHs from *T. pseudoethanolicus* and *T. brockii* by using site-directed mutagenesis and directed evolution are reviewed. Moreover, the thermal stability and organic solvent tolerance of these enzymes is illustrated by their concurrent inclusion in other interesting reactions to produce optically active alcohols and amines.

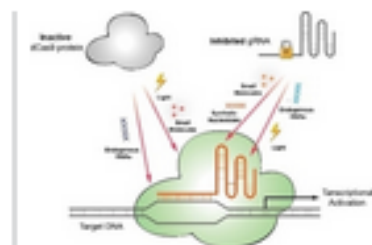
[Abstract](#) | [Full text](#) | [PDF](#) | [References](#) | [Request permissions](#)

Concepts

Inducible CRISPR-dCas9 Transcriptional Systems for Sensing and Genome Regulation

Han Wu, Prof. Fenglin Wang, Prof. Jian-Hui Jiang

Pages: 1894-1900 | First Published: 12 January 2021



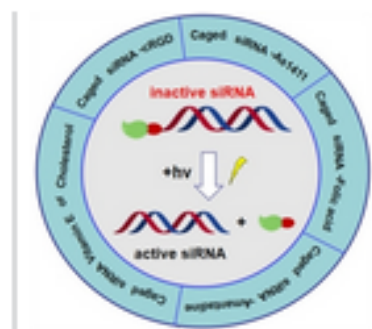
Transforming transcription: Inducible CRISPR-dCas9 transcription systems that rely on exogenous and endogenous cues to conditionally control the function of dCas9 proteins or gRNAs have provided pioneering platforms for genome engineering, cell-specific sensing and therapies.

[Abstract](#) | [Full text](#) | [PDF](#) | [References](#) | [Request permissions](#)

Photoregulation of Gene Expression with Ligand-Modified Caged siRNAs through Host/Guest Interaction

Dr. Qian Wang, Xinli Fan, Nannan Jing, Han Zhao, Dr. Lijia Yu, Prof. Xinjing Tang

Pages: 1901-1907 | First Published: 12 January 2021



Bigger cage, bigger effect: Photomodulation of gene expression has been successfully achieved *in vitro* and *in vivo* by using guest-molecule-modified caged siRNAs, which contains the corresponding bulky blocking complex at 5' terminus of the antisense RNA strand, through guest/host interactions.

[Abstract](#) | [Full text](#) | [PDF](#) | [References](#) | [Request permissions](#)

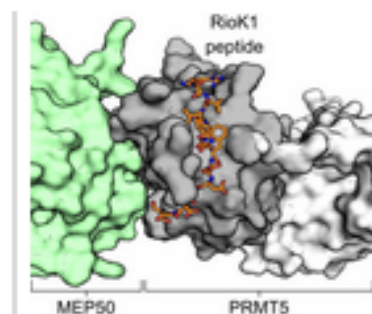
Communications

[Open Access](#)

Biochemical Investigation of the Interaction of p1Cin, RioK1 and COPR5 with the PRMT5-MEP50 Complex

Adrian Krzyzanowski, Dr. Raphael Gasper, Dr. H el ene Adihou, Dr. Peter T Hart, Prof. Dr. Herbert Waldmann

Pages: 1908-1914 | First Published: 24 February 2021



Determination of a PPI interface: The adaptor protein binding site of PRMT5 has been identified and studied by using synthetic peptides. A cocrystal structure of the PRMT5 TIM-barrel domain and a RioK1-derived peptide highlights the site of interaction.

[Abstract](#) | [Full text](#) | [PDF](#) | [References](#) | [Request permissions](#)

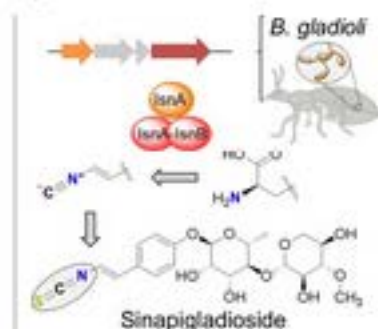
Very Important Paper

[Open Access](#)

Biosynthesis of Sinapigliadioside, an Antifungal Isothiocyanate from *Burkholderia* Symbionts

Benjamin Dose, Dr. Sarah P. Niehs, Dr. Kirstin Scherlach, Sophie Shahda, Dr. Laura V. Flores, Prof. Dr. Martin Kaltenpoth, Prof. Dr. Christian Hertweck

Pages: 1920-1924 | First Published: 19 March 2021



Alternative pathways: Genetic analyses and labeling studies provide the first insights into the biosynthesis of the rare isothiocyanate natural product sinapigliadioside from beetle-associated bacteria that might protect the beetle offspring against entomopathogenic fungi. Contrary to known isothiocyanate biosynthetic pathways, sinapigliadioside assembly involves an isonitrile synthase.

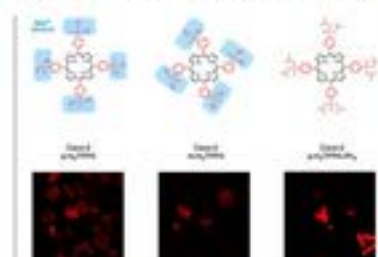
[Abstract](#) | [Full text](#) | [PDF](#) | [References](#) | [Request permissions](#)

[Open Access](#)

Arylphosphonate-Tethered Porphyrins: Fluorescence Silencing Speaks a Metal Language in Living Enterocytes

Dr. Claudia Keil, Julia Klein, Dr. Franz-Josef Schmitt, Dr. Yunus Zorlu, Prof. Dr. Hajo Haase, Dr. Gündoğ Yücesan

Pages: 1925-1931 | First Published: 07 February 2021



Pinpointing metals: Arylphosphonic acid fluorophores with a porphyrin core produced unique fluorescent behavior in response to each of the biologically significant metal ions studied. Thus they provide an expandable and engineerable platform for the development of improved, targeted fluorescence sensors suitable for in vivo applications to determine and visualize metals in tissues during disease progression.

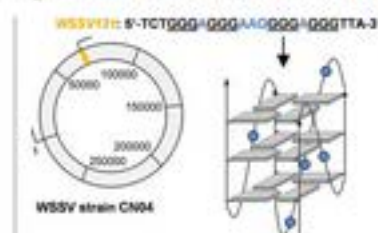
[Abstract](#) | [Full text](#) | [PDF](#) | [References](#) | [Request permissions](#)

[Open Access](#)

G-Quadruplex Formation in a Putative Coding Region of White Spot Syndrome Virus: Structural and Thermodynamic Aspects

Yvanes Maria Vianney, Dr. Maria Goretti M. Purwanto, Dr. Klaus Welsch

Pages: 1932-1935 | First Published: 12 March 2021



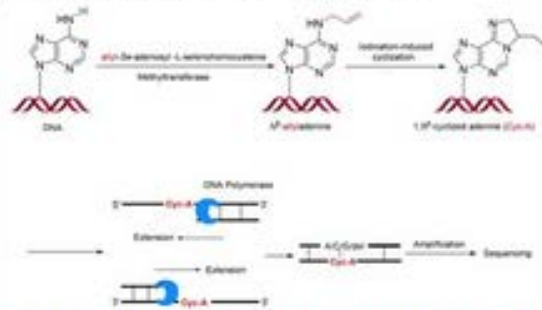
The right spot for white spot: A G-quadruplex-forming sequence identified within the DNA genome of white spot syndrome virus folds into a major and a thermodynamically less stable minor loop isomer. The parallel quadruplex scaffold might constitute a potential target for viral drug development against white spot disease.

[Abstract](#) | [Full text](#) | [PDF](#) | [References](#) | [Request permissions](#)

A Mutation-Based Method for Pinpointing a DNA N⁶-Methyladenine Methyltransferase Modification Site at Single Base Resolution

Mohan Cheng, Xiao Shu, Jie Cao, Minsong Gao, Siying Xiang, Prof. Fengqin Wang, Prof. Yizhen Wang, Prof. Jianzhao Liu

Pages: 1936-1939 | First Published: 28 March 2021



An enzyme-assisted chemical labeling method to pinpoint the DNA 6mA methyltransferase (MTase) substrate modification site at single-base resolution is described.

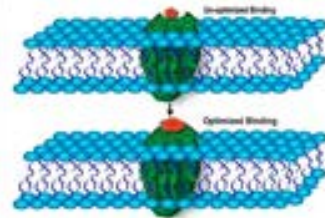
[Abstract](#) | [Full text](#) | [PDF](#) | [References](#) | [Request permissions](#)

Full Papers

Harnessing Multiple, Nonproteogenic Substitutions to Optimize CSP:ComD Hydrophobic Interactions in Group 1 *Streptococcus pneumoniae*

Tahmina A. Mily, Emilee R. Engler, Kylie S. Chichura, Alec R. Buttner, Dr. Bimal Koirala, Dr. Yftah Tal-Gan, Dr. Michael A. Bertucci

Pages: 1940-1947 | First Published: 28 February 2021



Unnaturally optimized: The use of unnatural amino acids allowed the optimization of hydrophobic interactions between CSP1 and the cognate ComD1 receptor by assessing how multiple, coordinated substitutions in the CSP1 amino acid sequence can affect CSP1 binding.

[Abstract](#) | [Full text](#) | [PDF](#) | [References](#) | [Request permissions](#)

Comparison of Two DNA Aptamers for Dopamine Using Homogeneous Binding Assays

Yaoyao Hou, Jianjun Hou, Dr. Xibei Liu

Pages: 1948-1954 | First Published: 30 March 2021



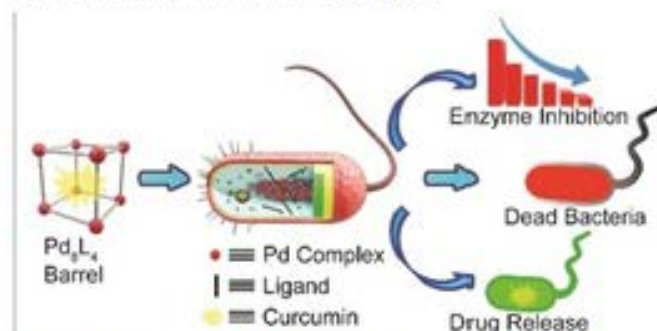
Two very different DNA aptamers have been reported for dopamine, one derived from an RNA aptamer (named Apt1) and other obtained via direct aptamer selection (named Apt2). In this study, we used four homogeneous binding assays to compare these two DNA dopamine aptamers. Apt1 does not appear to be able to bind dopamine specifically, while Apt2 showed specific binding and could be used for developing related biosensors.

[Abstract](#) | [Full text](#) | [PDF](#) | [References](#) | [Request permissions](#)

Supramolecular Interaction of Molecular Cage and β -Galactosidase: Application in Enzymatic Inhibition, Drug Delivery and Antimicrobial Activity

Avijit Mondal, Imtiaz Ahmad Bhat, Subbaraj Karunakaran, Dr. Minmoy De

Pages: 1955-1960 | First Published: 04 April 2021



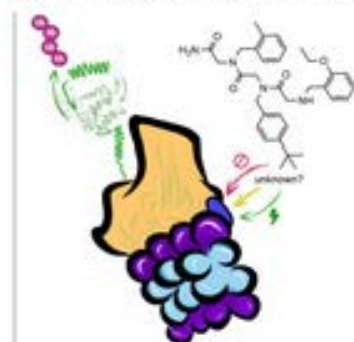
The effect of a water-soluble Pd₁₂⁰ molecular cage towards β -galactosidase enzyme activity was studied. The cage disintegrates in the presence of the enzyme and inhibits the enzyme by mixed mode of inhibition. This inhibition strategy and encapsulated hydrophobic curcumin inside the cage were used to control the growth of methicillin-resistant *Staphylococcus aureus*.

[Abstract](#) | [Full text](#) | [PDF](#) | [References](#) | [Request permissions](#)

Approaches to Evaluate the Impact of a Small-Molecule Binder to a Noncatalytic Site of the Proteasome

Wenzhi Tian, Marianne E. Maresh, Prof. Darci J. Trader

Pages: 1961-1965 | First Published: 22 February 2021



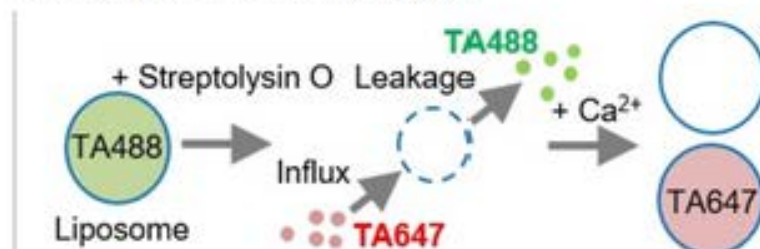
Investigating the impact of small molecules: There are a number of essential protein-protein interactions between the 19S regulatory particle and 20S core particle to form the full 26S proteasome. We investigated whether a small-molecule binder to Rpn-6, a 19S subunit, could disrupt 26S proteasome activity.

[Abstract](#) | [Full text](#) | [PDF](#) | [References](#) | [Request permissions](#)

Exchange of Proteins in Liposomes through Streptolysin O Pores

Dr. Gakushi Tsuji, Dr. Takeshi Sunami, Dr. Masaya Oki, Dr. Norikazu Ichihashi

Pages: 1966-1973 | First Published: 14 February 2021



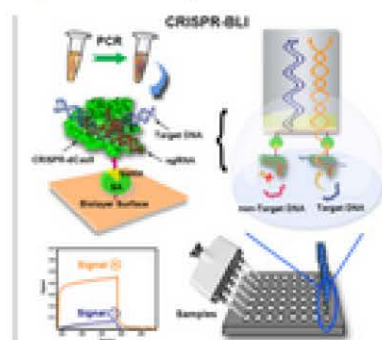
Taking a pore view of bioreactors: Streptolysin O creates pores in liposome membranes allowing proteins to permeate them. Enzymes including RNA polymerase can be supplied through these pores, allowing RNA to be synthesized in liposomes. The method could broaden the application of liposomes as biochemical reactors.

[Abstract](#) | [Full text](#) | [PDF](#) | [References](#) | [Request permissions](#)

Construction of a CRISPR-Biolayer Interferometry Platform for Real-Time, Sensitive, and Specific DNA Detection

Dr. Shan-Peng Qiao, Zhen-Ni Liu, Dr. Hai-Chao Li, Xin He, Hong Pan, Dr. Yu-Zhou Gao

Pages: 1974-1984 | First Published: 08 March 2021



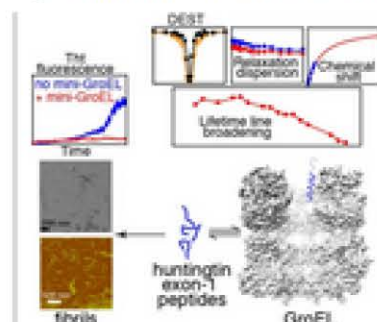
Threefold detection: A CRISPR biosensor is immobilized on a biolayer to construct a CRISPR-BLI platform for DNA detection. The CRISPR-BLI chip is rapid, label-free, and real-time, and has high sequence affinity and specificity due to the properties of BLI and the CRISPR probe. Coupling with PCR improves the sensitivity to 1.34 pg, revealing promising applications in dsDNA detection.

[Abstract](#) | [Full text](#) | [PDF](#) | [References](#) | [Request permissions](#)

Probing the Interaction of Huntingtin Exon-1 Polypeptides with the Chaperonin Nanomachine GroEL

Dr. Marielle A. Wälti, Dr. Samuel A. Kotler, Dr. G. Marius Clore

Pages: 1985-1991 | First Published: 28 February 2021



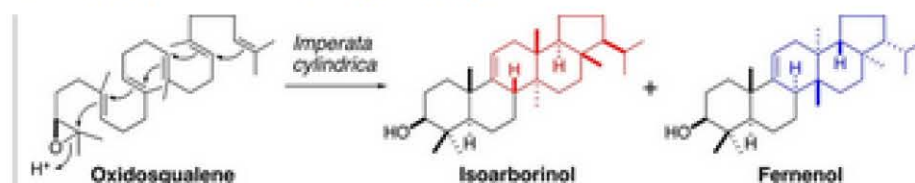
Polyglutamine expansion within the region of huntingtin encoded by exon-1 of the *htt* gene results in an aggregation-prone protein that accumulates in neuronal inclusion bodies. We show that the chaperonin GroEL, the bacterial homolog of human mitochondrial Hsp60, inhibits fibril formation of huntingtin exon-1 peptides and probe the interaction using NMR relaxation-based experiments designed to explore short-lived sparsely populated states.

[Abstract](#) | [Full text](#) | [PDF](#) | [References](#) | [Request permissions](#)

Two Triterpene Synthases from *Imperata cylindrica* Catalyzing the Formation of a Pair of Diastereoisomers through Boat or Chair Cyclization

Dr. Shingo Naraki, Mai Kakiyama, Sayuri Kato, Dr. Yusuke Saga, Dr. Kazuto Mannen, Dr. Shohei Takase, Dr. Akihito Takano, Sayaka Shimpo, Dr. Tsutomu Hosouchi, Dr. Takahisa Nakane, Dr. Hideyuki Suzuki, Dr. Tetsuo Kushiro

Pages: 1992-2001 | First Published: 04 March 2021



Controlling conformation during cyclization: *I. cylindrica* produces the diastereomeric triterpenes isoarborinol and femenol depending on whether the B-ring of oxidosqualene was in a boat or chair conformation during cyclization. Mutational studies on the two enzymes resulted in partial conversion of the products. Placing a histidine residue at a critical site resulted in the production of a rare triterpene.

[Abstract](#) | [Full text](#) | [PDF](#) | [References](#) | [Request permissions](#)